Instrument Science Report WFC3 2012-12 v.1.1

WFC3/UVIS Sky Backgrounds

Sylvia Baggett & Jay Anderson
June 28, 2012

ABSTRACT

This report summarizes the on-orbit background levels present in WFC3/UVIS full-frame images. The results are based on nearly all standard readout images taken since the installation of WFC3 on HST in May 2009, with a relatively small number of exclusions e.g. images with obvious anomalous backgrounds (such as extended targets filling the field of view) or those taken with the quad filters (different bandpass in each amp). Comparisons are provided to estimates from the Exposure Time Calculator (ETC). We anticipate these results to be helpful in fine-tuning the level of post-flash required to achieve the optimum balance of charge transfter efficiency (CTE) loss mitigation versus noise penalty. Observers considering the use of post-flash should refer to the White Paper (MacKenty & Smith 2012) on the CTE WWW page (http://www.stsci.edu/hst/wfc3/ins_performance/CTE/).

Introduction

Photometric monitoring of star fields as well as modeling of the WFC3 charge traps and their evolution over time has shown that images with low levels of background experience a proportionally larger amount of charge transfer efficiency (CTE) loss than images with high background levels (Noeske et al., 2012; Anderson, 2013). Specifically, low S/N sources embedded in low backgrounds (< ~10-15e-) lose a significant amount of charge to traps during readout while similar low S/N sources embedded in higher backgrounds (> 10-15e) are better able to retain charge during readout. The implication is that CTE losses, particularly for faint sources, can be mitigated by the presence of a relatively low background, achievable by lengthening exposure times to increase the natural background level and/or by applying a post-flash, a mode currently being commissioned for use on-orbit.

May 23, 2013: version 1.1., updated G280 predictions
June 28, 2012: version 1.0

The attainable background will be a key factor for observers in determining the optimum post-flash level needed. If the natural background will be at the level of 10's of electrons, as with some of the broader filters, then a post-flash will have limited benefit and may not be worth the noise penalty. However, for images with low sky backgrounds such as those taken with the UV or narrowband filters, a post-flash can provide significant CTE mitigation though to minimize the extra noise a post-flash will inject, the lowest optimum post-flash exposure level should be used. A knowledge of the natural observational background will enable fine-tuning of that post-flash level. For advice in using post-flash, please see the White Paper (MacKenty & Smith, 2012) on the CTE page (http://www.stsci.edu/hst/wfc3/ins_performance/CTE/).

Here we report on measured background values based on as large a set of UVIS full-frame archival data as possible, to allow observers to determine whether a post-flash would be necessary and if so, to choose the lowest effective flash level. For convenience, we also tabulate Exposure Time Calculator (ETC) background estimates under a variety of conditions but we recommend that observers use the ETC to confirm predicted background levels for their particular targets.

Data

The Mikulski Archive for Space Telescopes (MAST) was mined to identify all external WFC3/UVIS images taken since WFC3 was installed on HST (May 2009). From those, we selected all images taken in the standard observing mode used by the majority of observers: unbinned, full-frame, four-amp readouts. To capture the broadest set of observations, no distinction was made based on specific telescope pointings, target types, or observation date and time. Furthermore, no effort was made to exclude images taken under special observing conditions such as 1) LOW-SKY, with minimal zodiacal light (zodi) and earthshine, 2) SHADOW, with minimal geocoronal emission, 3) CVZ, which can contain relatively high backgrounds due to time spent grazing the bright earth-limb, or 4) parallels, images taken while another instrument, such as ACS or COS, is observing the primary target.

Exposures which *have* been excluded from the dataset are those where the background is known a priori as unlikely represent real sky, namely 1) external EARTH-CALs, which are calibration observations of the Earth, 2) images acquired with charge-injection mode, where 15,000 e- is injected into every Nth row, and 3) exposures taken with the quad filters, where each amp contains a different bandpass. Furthermore, known failed observations, e.g., a zero-length exposure, have been omitted, as well as any images with extremely high background values (>200 e-), typically indicative of bright extended targets filling the WFC3/UVIS field of view.

These criteria resulted in a set of more than 10,000 full-frame images; as discussed above, this does not represent all WFC3/UVIS images in the archive as by design, readout modes such as subarrays have been excluded. Table 1 below summarizes some of the dataset characteristics, listing filter name, description, pivot wavelength and width, followed by the number and percentage of full-frame images taken in that filter, the total exposure time, the average and standard deviation of the exposure times, as well as the median, minimum, and maximum exposure times. There are 41 full-field filters represented, including the UV grism; for two full-field filters, F631N and F845M, there were no images in the archive satisfying the criteria described above. The five filters with the highest usage in full-frame images to date have been F606W, F814W, F336W, F275W, and F350LP; more than half of this sample have used these five filters. The five least-used filters have been F689M, F280N, F953N, F763M, and F680N.

Table 1. Filter usage statistics based on all standard readout, full-frame unbinned images in the MAST archive, sorted by filter name; please refer to text for details of the selection criteria used to construct this sample set. Filter description, pivot wavelength, and width are taken from the WFC3 Instrument Handbook (Dressel, 2011).

Filter	Description	Pivot Wavel (nm)	Width (nm)	Num Imgs	Num Imgs (%)	Total Exptime (hrs)	Ave Exptime (sec)	Stdv Exptime (sec)	Median Exptime (sec)	Min Exptime (sec)	Max Exptime (sec)
F200LP	clear	488.3	502.2	118	1.2	8.0	244.1	228.5	120.	60.	758.
F218W	ISM feature	222.4	32.2	48	0.5	8.4	632.0	159.6	629.	5.	1000.
F225W	UV wide	235.9	46.7	298	2.9	57.7	697.4	335.0	680.	0.5	1476.
F275W	UV wide	270.4	39.8	1148	11.3	204.7	641.8	306.2	627.	3.6	1465.
F280N	MgII 2795/2802	283.1	4.3	10	0.1	2.8	1025.6	291.2	800.	800.	1364.
F300X	Wide UV	280.7	66.3	93	0.9	9.0	349.8	346.8	200.	1.	1461.
F336W	Stromgren u	335.5	51.1	1208	11.9	223.9	667.2	287.7	600.	0.5	1460.
F343N	[NeV] 3426	343.5	25.0	20	0.2	8.2	1470.2	46.9	1466.	1386.	1544.
F350LP	Long pass	584.6	475.8	715	7.0	113.9	573.4	225.2	490.	0.5	1300.
F373N	[OII] 3726/3728	373.0	5.0	25	0.2	6.6	945.8	371.5	900.	30.	1400.
F390M	CaII continuum	389.7	20.4	133	1.3	26.4	715.0	275.5	662.	50.	1544.
F390W	Washington C	392.1	89.6	391	3.8	70.3	647.4	436.1	620.	2.	1492.

F395N	CaII 3933/3968	395.5	8.5	28	0.3	5.3	681.8	386.3	697.	90.	1300.
F410M	Stromgren v	410.9	17.2	176	1.7	5.5	112.5	168.1	100.	5.	800.
F438W	WFPC2 B	432.5	61.8	353	3.5	52.2	532.7	359.4	410.	0.5	1534.
F467M	Stromgren b	468.3	20.1	102	1.0	23.6	833.1	618.2	500.	10.	1463.
F469N	HeII 4686	468.8	5.0	81	0.8	32.8	1458.1	248.6	1492.	400.	1561.
F475W	SDSS g	477.3	134.4	341	3.3	70.4	743.9	420.1	674.	1.5	1534.
F475X	Extra wide blue	493.9	205.6	116	1.1	12.7	393.4	246.9	360.	189.	1461.
F487N	Hβ 4861	487.1	6.0	37	0.4	8.2	794.5	282.2	800.	425.	1591.
F502N	[OIII] 5007	501.0	6.5	206	2.0	27.3	477.2	338.9	420.	1.2	1100.
F547M	Stromgren y	544.7	65.0	218	2.1	20.5	337.9	356.1	350.	4.	1459.
F555W	WFPC2 V	530.8	156.2	399	3.9	40.2	363.1	262.4	370.	0.5	1380.
F600LP	Long pass	744.4	229.2	332	3.3	51.0	552.5	236.5	571.5	194.	1461.
F606W	WFPC2 Wide V	588.7	218.2	1329	13.0	225.4	610.5	379.8	567.	2.9	1562.
F621M	11% passband	621.9	60.9	41	0.4	1.3	110.5	178.2	30.	30.	678.
F625W	SDSS r	624.2	146.3	141	1.4	19.2	490.8	258.6	414.	11.	1300.
F645N	continuum	645.4	8.4	23	0.2	2.7	427.8	59.1	410.	410.	615.
F656N	Hα 6562	656.1	1.8	64	0.6	11.2	629.2	354.9	660.	30.	1364.
F657N	Wide Hα+[NII]	656.7	12.1	79	0.8	12.4	563.8	257.4	530.	236.	1400.
F658N	[NII] 6583	658.4	2.8	41	0.4	6.3	555.2	234.5	500.	35.	1000.
F665N	z(Hα+[NII])	665.6	13.1	16	0.2	6.2	1391.4	291.0	1300.	1200.	2169.
F673N	[SII] 6717/6731	676.6	11.8	101	1.0	17.7	632.0	298.3	600.	15.	1443.
F680N	z(Hα+[NII])	687.7	37.1	3	<0.1	0.6	665.0	77.9	710.	575.	710.
F689M	11% passband	687.6	68.3	11	0.1	1.8	603.4	177.0	500.	500.	879.
F763M	11% passband	761.2	70.4	6	0.1	0.8	479.3	76.4	430.	430.	578.
F775W	SDSS i	764.7	117.1	152	1.5	19.5	462.3	257.2	503.5	3.	947.
F814W	WFPC2 Wide I	802.4	153.6	1257	12.3	218.9	627.0	402.7	600.	0.5	1670.
F850LP	SDSS z	916.6	118.2	63	0.6	4.3	248.3	189.9	340.	60.	750.

F953N	[SIII] 9532	953.0	9.7	7	0.1	1.6	807.1	73.2	850.	700.	850.
G280	UV grism	grism	N/A	262	2.6	34.7	477.2	175.9	400.	290.	950.

Analysis

The raw fits files as extracted from the archive were first processed through a Fortran routine to correct for the bias level using the overscan areas. In full-frame four-amp readouts, there are 25 columns of physical overscan on the left and right of each chip and 19 rows of physical overscan farthest from the amps. In addition, 30 columns of virtual overscan trail the science pixel columns associated with each quadrant. For this study, we measure a single overscan value based on all of the last 6 physical overscan rows, namely 6x2070 pixels; this avoids any possible settling issues which may be present in the first few rows of the overscan. The background measurements are performed quadrant by quadrant, using a sigma-clipped mean with a 3.5 sigma clipping. The values given in this report are averages of the four quadrants converted to electrons using the 1.5 e-/DN gain factor for WFC3.

The plot of background level as a function of exposure time for F438W is shown in Figure 1; for completeness, plots for all the filters have been included in the Appendix. The thin grey horizontal line marks the 10e- background level while the thick green line reflects a fit performed by eye to the lower envelope of the background levels. Since a natural range in sky is expected for on-orbit observations, we deliberately did not perform a fit to the minimum of each exposure bin, deeming it too conservative and not representative of typical background levels. Instead, we chose to perform a linear fit 'by eye' to estimate each filter's background in order to obtain a 'customary' value. The manual fit was fixed at 0.5 e- at the origin as most of the plots exhibited such an offset, due to a residual pedestal present between the science pixels and the overscan. Note that such a pedestal is removed during the standard pipeline processing using *calwf3*, which performs an overscan correction followed by a superbias correction.

The other lines in the figure are the representative ETC (version 20.1.1) cases as listed below; they all include a baseline dark current level of 5.4 e-/pix/hr.

Black solid line: average zodi, average earthshine, average airglow
Red dots: high (or low) zodi, average earthshine, average airglow
Blue dashes: average zodi, high earthshine, average airglow
Yellow dashes: average zodi, average earthshine, high airglow

Note that for many filters, the airglow contribution is neglible and thus the yellow dashes overlap the black solid line in the plots.

As can be seen in the figures, at each exposure time there are typically a large range of observed background values; the highest levels are attributed (and confirmed via spotchecks) to images containing rich starfields and/or extended nebular targets. However, even in images containing significant regions of relatively empty sky, the combination of zodi, earthshine, and/or the geocoronal line at 247.1nm will all contribute to the measured backgrounds and serve to scatter points upwards in the figures.

For the majority of filters, the ETC values bracket the lower envelope of the measured backgrounds quite well; in addition, either the low zodi or the average ETC values are in good agreement with the manual fits to the observations. However, in several filters (e.g., F225W, F275W, F300X) the ETC values are higher than the observations and in several filters (e.g. F656N, F658N) the ETC values are lower than the observations. This mismatch is likely due to the very low levels of background in these filters, where there is effectively no sky and the primary component arises from dark current. There are some filters where the ETC and manual fits do not match well (e.g. F665N, F680N, F763M) but in these cases the manual fits should be considered highly suspect as there are very few observations from which to make an assessment.

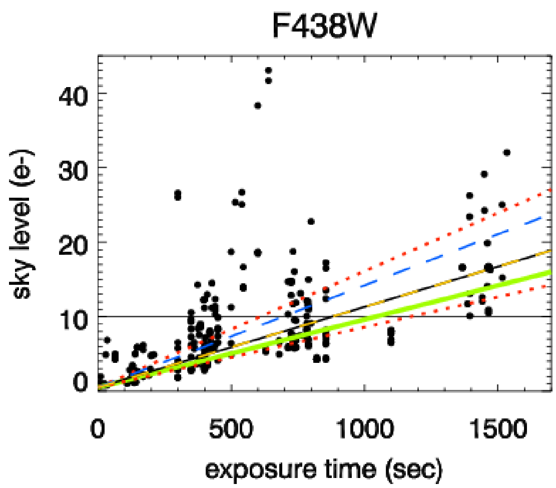

Figure 1. Background levels as a function of exposure time for F438W full-frame images (filled circles). The horizontal grey line marks the 10e- background level and the thick green line denotes a manual fit to the lower boundary of the background level distribution. Other lines mark ETC values: red dotted, blue dashed, and yellow dashed are the zodi background (high and low), high earthshine, and high airglow, respectively. The average background is shown with a solid black line; for this filter, it appears dashed due to overlap with the airglow line.

In Table 2 we summarize the results from our manual fits in the form of the measured slope (x1000) and the exposure time required to achieve 10e- background. In addition, for convenience we tabulate the ETC estimates shown in the figures in the Appendix: low and high zodi, high earthshine, and high airglow sky levels, given in e-/pix for a 1000 sec exposure. These values include the dark current, currently set in the ETC as 5.4 e-/pix/hr (1.5 e-/pix in 1000 sec). The dark was only ~2 e-/pix/hr at launch (2009) and due to radiation damage on-orbit, has gradually increased to ~6 e-/pix/hr (mid-2012). As can be seen in Table 2, there are 15 filters, long-pass and wide-band of course but also some medium-bandpass, for which observed background levels of ~10e- are seen in 1000 sec exposures; these are highlighted with dark grey in the table. Extending exposure times to 2000 sec results in five more filters – including the two narrowbands F673N and F657N - with sky backgrounds typically >10e- (light grey in the table).

There are, however, 21 filters, notably most UV filters as well as medium and narrowband filters, which show ~3 e- or less of background (sky+dark) in 1000 sec exposures. Observers preparing proposals with these filters, particularly for targets with low S/N, will want to consider adding a low-level post-flash exposure via the FLASH optional parameter (APT Phase II Proposal Instructions, 2012). The parameter controls the number of electrons which will be added to the image via the post-flash LED (light-emitting diode). Note that this value represents an average flash level as the LED illumination pattern exhibits gradients of +/-20% across the full WFC3/UVIS field of view (Baggett & Wheeler, 2012). Based on the limited data available, the post-flash pattern is stable to 1%. The smallest level of post-flash should be applied, enough to achieve sufficient total background (sky + post-flash) to provide CTE mitigation yet low enough to minimize the additional noise added by the flash. For the most current value of the optimum total background to achieve this balance (expected to be 10-15e-), please see the White Paper (MacKenty & Smith, 2012).

Table 2. Estimated background levels (sky + dark) in full-frame UVIS images. Highlighted rows mark those filters with backgrounds measured from archival images typically 10e- or more in 1000sec (dark grey) and 10e- or more in 2000 sec (light grey).

	Observation-based		Exposure Time Calculator (ETC v.20.1.1)				
Filter	Slope of manual fit X1000	Exptime to reach 10e- (sec)	Average in 1000 sec (e-/pix)	Low zodi level in 1000 sec (e-/pix)	High zodi level in 1000 sec (e-/pix)	High earthshine in 1000 sec (e-/pix)	High airglow in 1000 sec (e-/pix)
f200lp	79.5	125.8	105.6	75.8	161.6	135.3	110.7
f218w	0.8	12142.9	0.1	1.6	1.6	1.6	1.7
f225w	1.0	10000.0	1.0	2.5	2.6	2.5	3.5

f275w	1.0	10000.0	0.8	2.2	2.5	2.3	2.8
f280n	1.5	6538.5	~0.0	1.5	1.5	1.5	1.5
f300x	1.5	6800.0	2.8	4.0	4.9	4.4	6.2
f336w	4.5	2207.8	2.1	2.9	4.9	3.9	3.6
f343n	1.5	6800.0	1.2	2.3	3.4	2.9	2.7
f350lp	89.7	111.5	105.2	74.6	162.6	136.2	106.7
f373n	2.1	4857.2	0.3	1.7	1.9	1.8	1.8
f390m	2.4	4250.0	2.6	2.6	3.9	3.6	3.1
f390w	9.1	1096.8	9.4	8.1	15.8	13.7	10.9
f395n	2.9	3400.0	0.7	2.0	2.6	2.5	2.2
f410m	3.8	2615.4	2.6	3.3	5.4	4.9	4.1
f438w	9.1	1096.8	9.3	8.1	15.6	13.7	10.8
f467m	3.8	2615.4	4.3	4.5	8.0	7.1	5.8
f469n	1.8	5666.7	0.7	2.0	2.6	2.5	2.2
f475w	19.1	523.1	26.3	20.0	41.2	35.8	27.8
f475x	29.1	343.4	42.3	31.2	65.6	56.5	43.8
f487n	3.5	2833.3	1.1	2.3	3.2	2.9	2.6
f502n	2.5	4047.6	1.3	2.4	3.4	3.2	2.8
f547m	12.9	772.7	14.2	11.4	23.0	19.9	15.7
f555w	35.0	285.7	35.9	26.8	56.2	48.3	37.5
f600lp	37.9	263.6	57.3	40.9	89.9	74.0	58.8
f606w	37.9	263.6	55.1	40.0	85.6	72.5	56.6
f621m	13.9	717.9	15.9	12.5	25.8	21.8	17.4
f625w	29.1	343.4	36.5	26.9	57.3	48.3	38.0
f631n	N/A	N/A	N/A	0.9	2.0	1.7	1.3

f645n	2.9	3400.0	1.9	2.8	4.4	3.9	3.4
f656n	3.2	3090.9	0.4	1.7	2.1	2.0	1.9
f657n	5.0	2000.0	2.8	3.4	5.8	5.1	4.3
f658n	3.4	2956.5	0.6	1.9	2.5	2.3	2.1
f665n	2.4	4250.0	3.1	3.6	6.2	5.4	4.6
f673n	6.2	1619.0	2.7	3.4	5.6	4.9	4.2
f680n	4.3	2328.8	8.5	7.4	14.6	12.3	10.0
f689m	13.5	739.1	15.4	12.2	25.2	21.1	16.9
f763m	8.6	1164.4	13.0	10.5	21.6	18.0	14.5
f775w	21.5	465.8	23.6	17.7	38.0	31.3	25.1
f814w	23.2	430.4	30.1	22.1	48.1	39.4	31.6
f845m	N/A	N/A	N/A	6.4	14.5	11.7	9.3
f850lp	11.5	871.8	8.8	7.5	15.2	12.5	10.3
f953n	2.4	4250.0	0.4	1.8	2.1	2.0	1.9
g280	55.0	181.8	100.7	71.3	151.8	127.2	104.1

For further details of the HST backgrounds, we refer the interested reader to several other sources of information. First, the WFC3 ETC (Exposure Time Calculator) provides a means to compute a predicted total background based upon observing mode, target location and/or observing season as well as a means to specify the desired normalization of zodiacal light, earthshine, and airglow contributions. The report by Giavalisco et al. (2002) documents the spectral models of the HST background which have been used to populate the ETC databases. More generally, the WFC3 Instrument Handbook summarizes earthshine and zodiacal light levels as a function of wavelength, zodiacal light as a function of ecliptic latitude and longitude, and the contributions of the Moon and sunlit Earth as a function of the angle between the target and the Earth or Moon (Section 9.7, Version 4.0, Dressel 2011).

Conclusions

We have presented on-orbit background measurements based on all WFC3/UVIS unbinned full-frame images taken since launch, useful for optimizing the post-flash level if needed. About half of the filters have sky levels >10 e- in exposures of 2000 sec or longer and thus may have sufficient natural background to mitigate CTE without requiring a post-flash as the "sweet spot" is expected to be 10-15 e-. The remaining filters, mostly UV plus some medium and narrowband filters, will have background levels <3e- in 1000 sec exposures and a low-level post-flash should be considered as a means of boosting the total background to the optimum level. At the optimized background level, observers will be able to mitigate most of the CTE losses, particularly for low S/N targets which suffer a proportionately larger loss than brighter sources, yet minimize the additional noise contributed by the flash. For advice on whether to use post-flash and how to choose the optimum level, please see the White Paper (MacKenty & Smith, 2012) on the CTE WWW page at http://www.stsci.edu/hst/wfc3/ins_performance/CTE/.

Acknowledgements

We thank Linda Smith whose review improved this manuscript.

Note for Version 1.1

May 23, 2013. An error in presenting the G280 ETC background predictions has been corrected in the grism entry in Table 2 as well as the corresponding plot in Appendix A. The problem was the result of using an incorrect aperture size for the grism when running the ETC. The measured background levels from the on-orbit grism images are unaffected by the error and remain unchanged. Background levels, both predicted and observed, for all standard UVIS filters remain unchanged. We thank L. Dressel, J. Lee, and N.Pirzkal for helpful discussions which led to the resolution of the issue.

References

Anderson, J., 2013, "Fitting a Pixel-based Model to a CCD Detector: WFC3/UVIS and Low-Background Issues," in prep.

Baggett, S., & Wheeler, T., "WFC3/UVIS TV3 Post-Flash Results," STScI Technical Instrument Report 2012-01. Copies are available upon request to help@stsci.edu.

Dressel, L., 2011, "Wide Field Camera 3 Instrument Handbook, Version 4.0", (Baltimore: STScI).

Giavalisco, M., Sahu, K., and Bohlin, R., "New Estimates of the Sky Background for the HST Exposure Time Calculator," WFC3 Instrument Science Report 2002-12.

Noeske, K., Baggett, S., Bushouse, H., Petro, L., Gilliland, R., and Khozurina-Platais, V., "UVIS Charge Transfer Efficiency October 2009 to October 2011," WFC3 Instrument Science Report 2012-09.

HST Phase II Proposal Instructions for Cycle 20, June 2012, http://www.stsci.edu/ftp/documents/p2pi/p2pi.pdf

MacKenty, J., & Smith, L., CTE White Paper, in prep, 2012. http://www.stsci.edu/hst/wfc3/ins_performance/CTE/.

Appendix A.

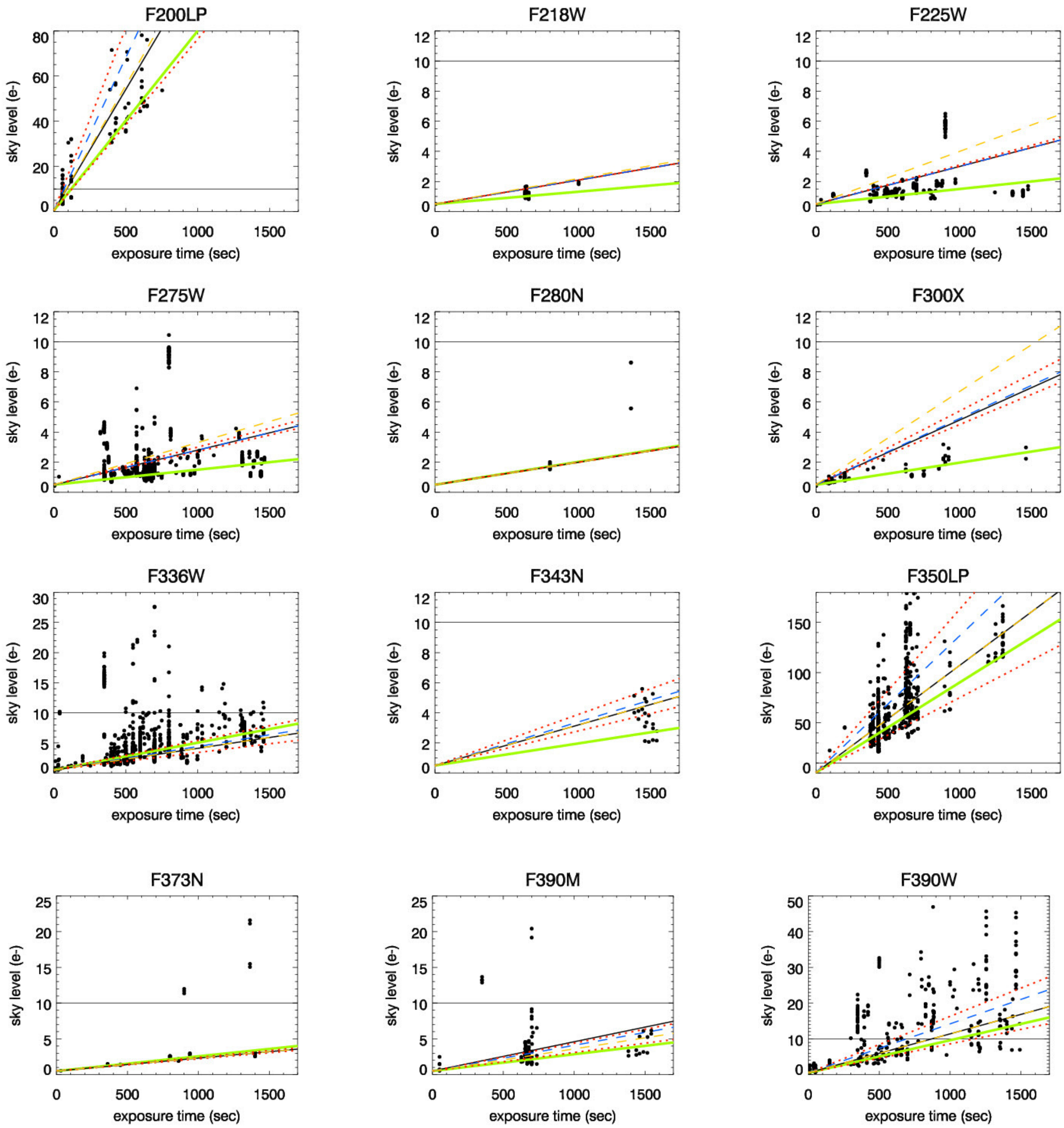

Figure 2a. Background levels as a function of filter and exposure time for unbinned full-frame images (filled circles). The horizontal grey line marks the 10e- background level and the thick green line denotes a manual fit to the lower boundary of the background level distribution. The solid black line, red dotted lines, blue and yellow dashed lines denote ETC values: the average background, high and low zodiacal background, high earthshine, and high airglow, respectively.

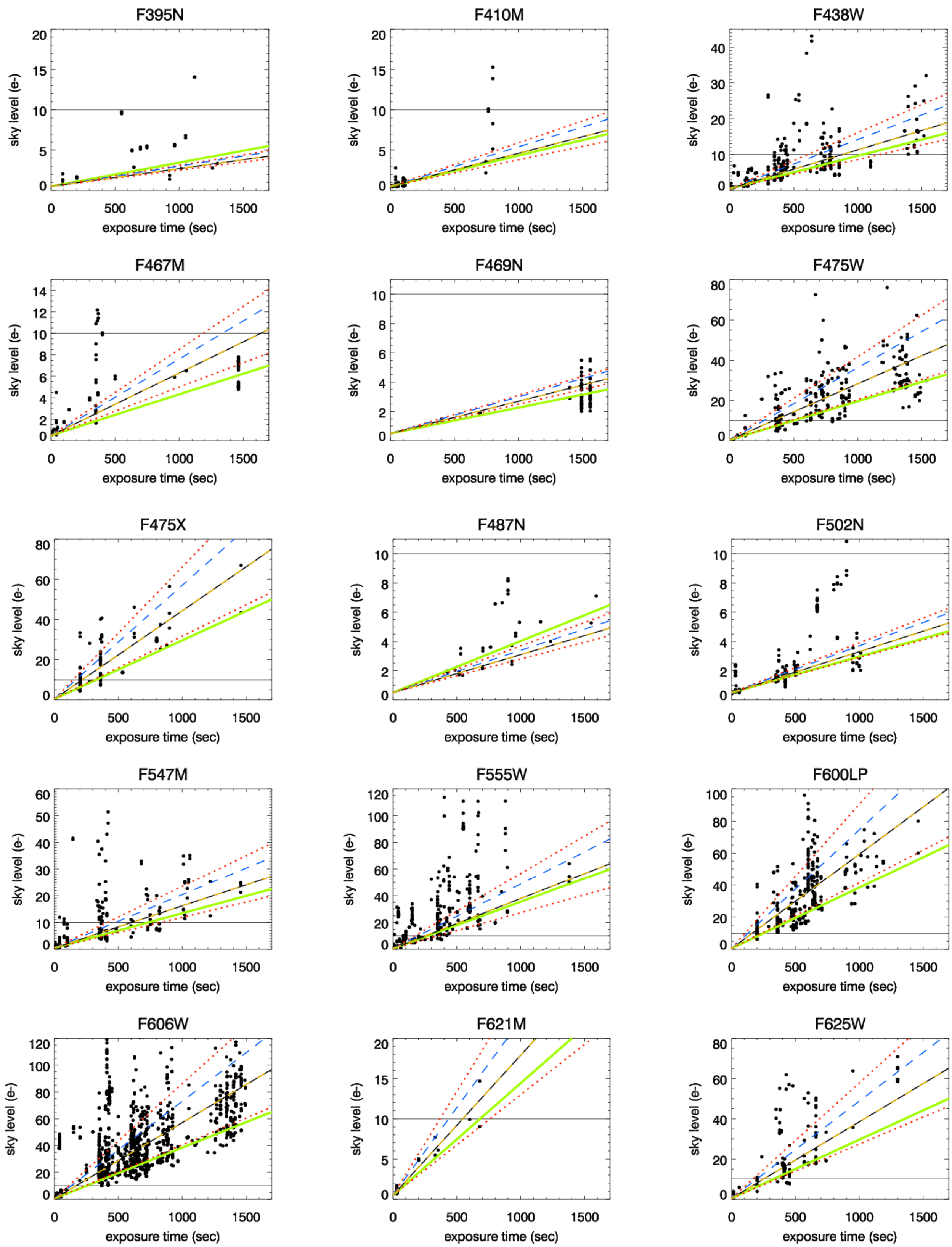

Figure 2b. Same as for 2a.

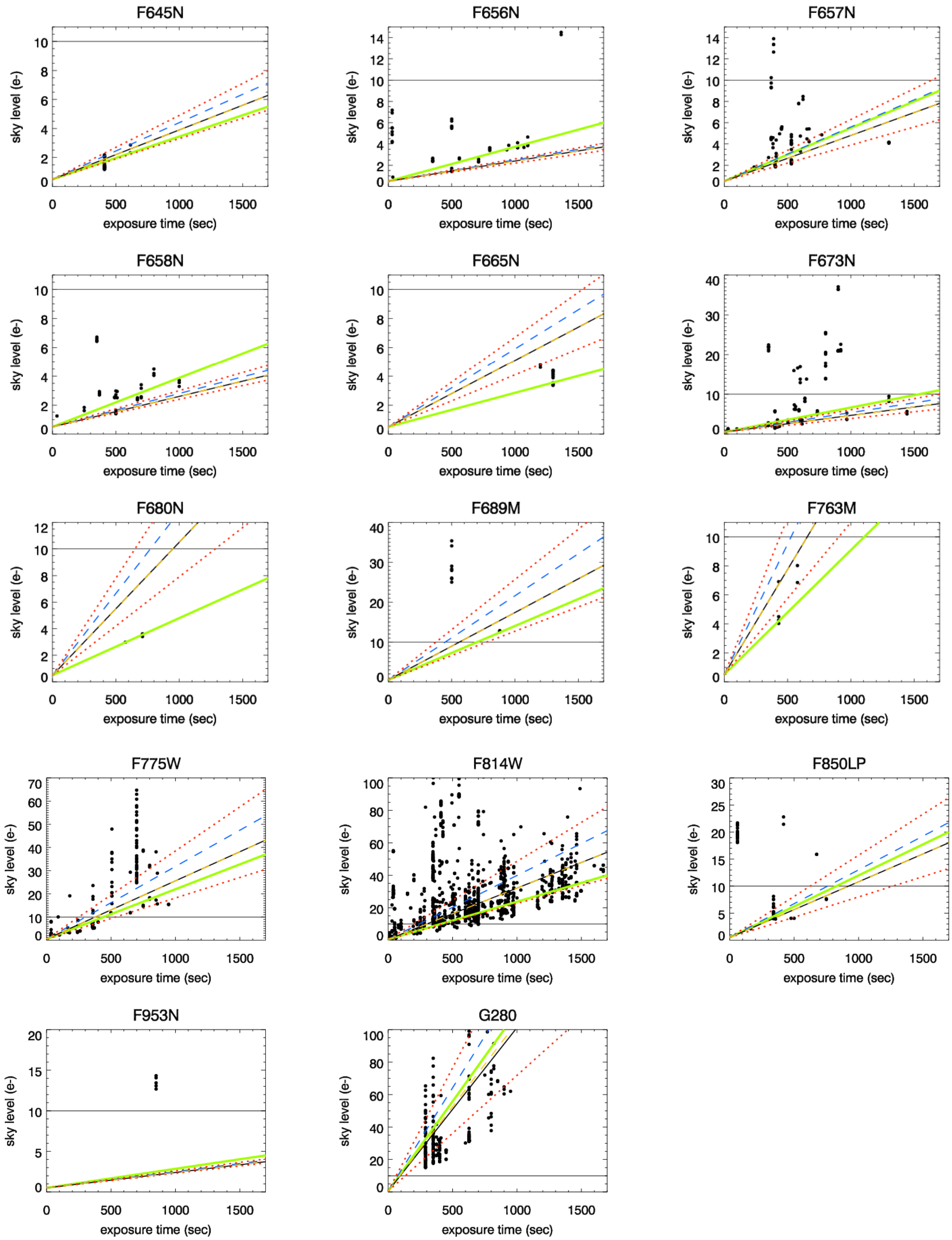

Figure 2c. Same as for 2a.